

SSNV231 – Sphere digs under internal pressure in great deformations

Summary:

The objective of this test is to validate the various incompressible formulations in great deformations. The advantage of this case test is that one has an analytical solution. Five modelings are used to validate the formulations whatever the type of finite element:

Modeling a: quadratic 3D grid HEXA20 (INCO_UPG, INCO_UP)
Modeling b: quadratic 3D grid TETRA10 (INCO_UPG, INCO_UP)
Modeling C: quadratic 3D grid PENTA15 (INCO_UPG, INCO_UP)
Modeling D: Quadratic AXIS grid QUAD8 (INCO_UPG, INCO_UP)
Modeling E: Quadratic AXIS grid TRIA6 (INCO_UPG, INCO_UP)

1 Problem of reference

1.1 Geometry

One considers a hollow sphere of external ray 1 m and of internal ray 0.2 m .

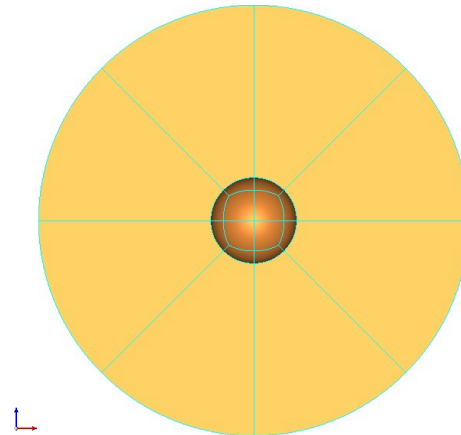


Figure 1.1-a : Cut of the studied sphere

1.2 Properties of material

The material has a perfectly plastic elastoplastic behavior. Its surface of load east defines by the criterion of von Mises. The properties materials are:

- $E = 200\,000\text{ MPa}$
- $\nu = 0.3$
- $\sigma_y = 150\text{ MPa}$

1.3 Boundary conditions and loadings

One applies an internal pressure until reaching the whole plasticization of the sphere. External surface is free of effort.

1.4 Initial conditions

Nothing

2 Reference solution

2.1 Method of calculating

In what follows, all the sizes defined in the initial configuration will be written in capital letters. The sizes defined in the deformed configuration will be written in small letters.

To establish the analytical solution, one considers a sphere of initial rays interior A and outside B . The material is elastoplastic with perfect plasticity. The plastic flow normal and is associated with the criterion of von Mises, of elastic limit σ_y . Elasticity isotropic is defined by the modules of compressibility and shearing, K and μ . The sphere is subjected to an internal pressure P .

Being given the spherical symmetry of the geometry and loading, one seeks a solution which presents the same properties of invariance what excludes the research solution forked. The solution depends only on the distance to the center of the noted sphere R in the initial configuration and r in the deformed configuration. Displacement is purely radial: $\vec{u}(r) = u(r)\vec{e}_r$, where $(\vec{e}_r, \vec{e}_\theta, \vec{e}_\varphi)$ is the orthonormal base associated with the spherical frame of reference. The definition of the operators will thus be used grad , div , ... adequate. The tensor of the constraints is expressed in the following way:

$$\sigma = \sigma_{rr}(r)\vec{e}_r \otimes \vec{e}_r + \sigma_{\theta\theta}(r)(\vec{e}_\theta \otimes \vec{e}_\theta + \vec{e}_\varphi \otimes \vec{e}_\varphi) \quad (1)$$

Concerning displacement, its expression in the configuration of reference is: $\vec{u}(\vec{X}) = U(R)\vec{e}_r$. One can notice that, by definition, one has the relations:

$$r = R + U(R) \text{ and } u(r) = U(R)$$

One from of deduced the following formula for the derivative

$$\frac{\partial U}{\partial R} = \frac{\partial u}{\partial r} \frac{\partial r}{\partial R} = \frac{\partial u}{\partial r} \left(1 + \frac{\partial U}{\partial R} \right) \Rightarrow \frac{\partial U}{\partial R} = \frac{\frac{\partial u}{\partial r}}{\left(1 - \frac{\partial u}{\partial r} \right)} \quad (2)$$

The gradient of the transformation is calculated:

$$\mathbf{F} = \left(1 + \frac{\partial U}{\partial R} \right) \vec{e}_r \otimes \vec{e}_r + \left(1 + \frac{U}{R} \right) (\vec{e}_\theta \otimes \vec{e}_\theta + \vec{e}_\varphi \otimes \vec{e}_\varphi) \quad (3)$$

Note:

\mathbf{F} admits constant clean directions during the transformation.

The deformation logarithmic curve admits then simply like expression:

$$\mathbf{E} = \ln \left(1 + \frac{\partial U}{\partial R} \right) \vec{e}_r \otimes \vec{e}_r + \ln \left(1 + \frac{U}{R} \right) (\vec{e}_\theta \otimes \vec{e}_\theta + \vec{e}_\varphi \otimes \vec{e}_\varphi) \quad (4)$$

Note:

In this case, typical case the rate of deformation $\dot{\mathbf{E}}$ coincide with the rate of Eulérien deformation $\dot{\mathbf{D}}$, so that the tensor of constraint \mathbf{T} associated with the deformations logarithmic curves is equal to the content of Kirchhoff $\boldsymbol{\tau}$. It is a favorable situation to display an analytical solution.

In the deformed configuration, the deformation $e(\vec{x})=E(\vec{X})$ express yourself:

$$e = -\ln\left(1 - \frac{\partial u}{\partial r}\right) \vec{e}_r \otimes \vec{e}_r + (\ln r - \ln(r-u)) (\vec{e}_\theta \otimes \vec{e}_\theta + \vec{e}_\varphi \otimes \vec{e}_\varphi) \quad (5)$$

It is also useful to express Jacobien of the transformation and its logarithm in the deformed configuration:

$$j = \det F = \frac{1}{\left(1 - \frac{\partial u}{\partial r}\right)} \left(\frac{r}{r-u}\right)^2 \quad \text{and} \quad \ln j = -\ln\left(1 - \frac{\partial u}{\partial r}\right) + 2 \ln r - 2 \ln(r-u) = \text{tr } e \quad (6)$$

The equilibrium equations can be also expressed in the configuration deformed according to the tensor of Kirchhoff $\tau = j \sigma$:

$$\text{div}_x \left(\frac{\tau}{j} \right) = \mathbf{0} \Leftrightarrow \frac{\partial \tau_{rr}}{\partial r} - \tau_{rr} \frac{\partial \ln j}{\partial r} + \frac{2}{r} (\tau_{rr} - \tau_{\theta\theta}) = 0 \quad (7)$$

Moreover, one has the boundary conditions:

$$\tau_{rr}(b) = 0 \quad \text{and} \quad \tau_{rr}(a) = j(a)P \quad (8)$$

Where a and b are the rays interior and outside of the deformed sphere. Account held of spherical symmetry, it is equivalent to impose an internal pressure or a radial displacement on the interior skin. One will prefer to control calculation in displacement, so that the second boundary condition is replaced by:

$$u(a) = U^{imp} \quad (9)$$

As regards the behavior, the hydrostatic part is purely elastic:

$$\text{tr } \tau = 3K \text{tr } e \Leftrightarrow 3K \ln j = \tau_{rr} + 2\tau_{\theta\theta} \quad (10)$$

For the deviatoric part, there are the relations classic of the plasticity of von Mises:

$$\tau_{eq} \leq \sigma_y; \dot{p} \geq 0; \dot{p}(\tau_{eq} - \sigma_y) = 0 \quad (11)$$

$$\tau^D = 2\mu(e^D + e^p) \quad \text{and} \quad \dot{e}^p = \frac{3}{2} \dot{p} \frac{\tau^D}{\tau_{eq}} \quad (12)$$

As regards answer of the structure, one expects a scenario in which the plastic zone gradually develops interior towards the outside of the sphere. When it reaches the external wall, all the points of the sphere are in plastic mode is:

$$\tau_{eq} = \sigma_y \Leftrightarrow \tau_{\theta\theta} - \tau_{rr} = \sigma_y \quad (13)$$

Moreover, at the time when the external wall is reached, the plastic deformation is still worthless there. One thus has:

$$e^D(b) = \frac{1}{2\mu} \tau^D(b) \Leftrightarrow \frac{(\tau_{rr}(b) - \tau_{\theta\theta}(b))}{2\mu} = \ln \left(\frac{1 - \frac{\partial u}{\partial r}}{r-u} \right) \Big|_b + \ln b \quad (14)$$

When the plastic zone leads to the external wall, one of the two components of the tensor of the constraint is known in any point via (13). The relation of balance (7) as well as the spherical part of the behavior (10) then make it possible to entirely determine the stress field, as well as Jacobien of the transformation. In fact, contrary to the case of the small deformations, these two equations are coupled. They are written:

$$\begin{cases} \frac{\partial \tau_{rr}}{\partial r} - \tau_{rr} \frac{\partial \ln j}{\partial r} + \frac{2}{r} (\tau_{rr} - \tau_{\theta\theta}) = 0 \\ 3K \ln j = \tau_{rr} + 2\tau_{\theta\theta} \end{cases} \quad (15)$$

In substituent the definition of $\ln j$ in the first equation of (15), one obtains:

$$\frac{\partial}{\partial r} \left(\tau_{rr} - \frac{\tau_{rr}^2}{2K} \right) = \frac{2}{r} \sigma_y \quad (16)$$

This equation is integrated easily by taking of account the boundary condition (8)

$$\tau_{rr} - \frac{\tau_{rr}^2}{2K} = 2\sigma_y \ln \left(\frac{r}{b} \right) \quad (17)$$

The stress field can be deduced by solving this equation from the second order. The choice of the root is fixed by the fact that it is about a compressive stress, therefore negative. The field of change of volume $\ln j$ from of deduced then through (15):

$$\begin{cases} \tau_{rr}(r) = K - \sqrt{K^2 - 4K\sigma_y \ln \left(\frac{r}{b} \right)} \\ \ln j(r) = 1 - \sqrt{1 - 4\frac{\sigma_y}{K} \ln \left(\frac{r}{b} \right)} + \frac{2\sigma_y}{3K} \end{cases} \quad (18)$$

In addition, the kinematic relation (6) can be rewritten:

$$\frac{\partial}{\partial r} ((r-u)^3) = \frac{3r^2}{\exp \ln j} \quad (19)$$

By taking of account the definition $b-u(b) = B$, one from of deduced by integration:

$$(r-u)^3 = B^2 - \int_r^b \frac{3\rho^2}{\exp \ln j(\rho)} d\rho \quad (20)$$

The primitive in (20) will have to be calculated numerically.

One can be also based on the relation (19) to simply express the ray deformed in b . Indeed, in $r=b$, the change of volume is worth:

$$\ln j(b) = \frac{2\sigma_y}{3K} \quad (21)$$

The equation (19) is written in $r=b$:

$$\left(1 - \frac{\partial u}{\partial r}\right) = \frac{b^2}{B^2} \exp\left(-\frac{2\sigma_y}{3K}\right) \quad (22)$$

The condition of continuity (14) then allows to fix the ray of the deformed sphere because it is still expressed:

$$\left(1 - \frac{\partial u}{\partial r}\right) = \left(\frac{b}{B}\right)^{-1} \exp\left(\frac{\sigma_y}{2\mu}\right) \quad (23)$$

From (22) and (23), one deduces the external ray deformation:

$$\frac{b}{B} = \exp\left(\frac{\sigma_y}{3} \left(\frac{1}{2\mu} + \frac{2}{3K}\right)\right) \quad (24)$$

The knowledge of the strain and the stress makes it possible to determine in its turn the field of cumulated plastic deformation p , Indeed, its evolution is controlled by the tensorial equation (12). More precisely, it proves that the direction τ^D/τ_{eq} is constant what makes it possible to integrate the plastic deformation simply:

$$e^p = p \left(\vec{e}_r \otimes \vec{e}_r - \frac{1}{2} \vec{e}_\theta \otimes \vec{e}_\theta - \frac{1}{2} \vec{e}_\varphi \otimes \vec{e}_\varphi \right) \quad (25)$$

Then in substituent this expression in the first equation of (12), one from of deduced:

$$p(r) = \frac{2}{3} (e_{\theta\theta} - e_{rr}) - \frac{\sigma_y}{3\mu} = \frac{2}{3} \left(\ln r - \frac{\sigma_y}{2\mu} + \ln \frac{1 - \frac{\partial u}{\partial r}}{r - u} \right) \quad (26)$$

Where the expression of the field of displacement is henceforth known according to (20).

Finally, the interior boundary condition makes it possible to determine the critical level of loading for which the plastic zone reaches the external wall. Indeed, the interior ray déformée is given in an implicit way by the relation (20) precisely expressed in $r=a$:

$$\int_r^b \frac{3\rho^2}{\exp \ln j(\rho)} d\rho = B^3 - A^3 \quad (27)$$

2.2 Sizes and results of reference

The reference variables are the trace of the constraint and the plastic deformation cumulated in configuration deformed for the points of Gauss having the R smallest and largest.

2.3 Uncertainties on the solution

The solution being analytical, there is not uncertainty.

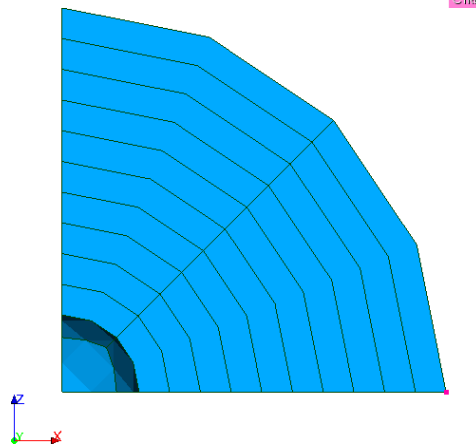
2.4 Bibliographical references

- 1 E. LORENTZ, "Dualisation of the conditions of quasi-incompressibility", Document interns EDF R & D, 2011.

3 Modeling A

3.1 Characteristics of modeling

One takes advantage of symmetries of the problem to model only one eighth of the sphere.



Three modelings are tested: 3D_INCO_UPG (SIMO_MIEHE and GDEF_LOG) and 3D_INCO_UP

3.2 Characteristics of the grid

The grid of 246 nodes contains 30 elements of the type HEXA20.

3.3 Sizes tested and results

One tests the trace of the constraints and the plastic deformation cumulated for the points of the excentré Gauss and excentré.

MODELISATION=' 3D_INCO_UPG ' and DEFORMATION=' SIMO_MIEHE '

Identification	Type of reference	Value of reference	Tolerance
Not the excentré Gauss - $tr\sigma$ - Pa	'ANALYTICAL'	-1039159346.8	0.3%
Not the excentré Gauss - $tr\sigma$ - Pa	'ANALYTICAL'	280042736.64	2%
Not the excentré Gauss - p	'ANALYTICAL'	0.13857481948	30%
Not the excentré Gauss - p	'ANALYTICAL'	7.5327100205e ⁻⁵	45%

MODELISATION=' 3D_INCO_UPG ' and DEFORMATION=' GDEF_LOG '

Identification	Type of reference	Value of reference	Tolerance
Not the excentré Gauss - $tr\sigma$ - Pa	'ANALYTICAL'	-1039075543.3	0.3%
Not the excentré Gauss - $tr\sigma$ - Pa	'ANALYTICAL'	280042663.38	2%
Not the excentré Gauss - p	'ANALYTICAL'	0.13853470251	30%
Not the excentré Gauss	'ANALYTICAL'	7.5327415674e ⁻⁵	45%

Warning : The translation process used on this website is a "Machine Translation". It may be imprecise and inaccurate in whole or in part and is provided as a convenience.

Copyright 2019 EDF R&D - Licensed under the terms of the GNU FDL (<http://www.gnu.org/copyleft/fdl.html>)

- p			
-----	--	--	--

MODELISATION=' 3D_INCO_UP' and DEFORMATION=' GDEF_LOG'

Identification	Type of reference	Value of reference	Tolerance
Not the excentré Gauss - $tr\sigma$ - Pa	'ANALYTICAL'	-1039075544	0.3%
Not the excentré Gauss - $tr\sigma$ - Pa	'ANALYTICAL'	280042663.37	2%
Not the excentré Gauss - p	'ANALYTICAL'	0.13853470247	30%
Not the excentré Gauss - p	'ANALYTICAL'	7.5327415705e ⁻⁵	45%

3.4 Remarks

All the incompressible formulations give good performances. One can see on Figure 3.4-a that one does not have any more oscillations on the value of the trace of the constraints with the incompressible formulations contrary to the standard elements 3D.

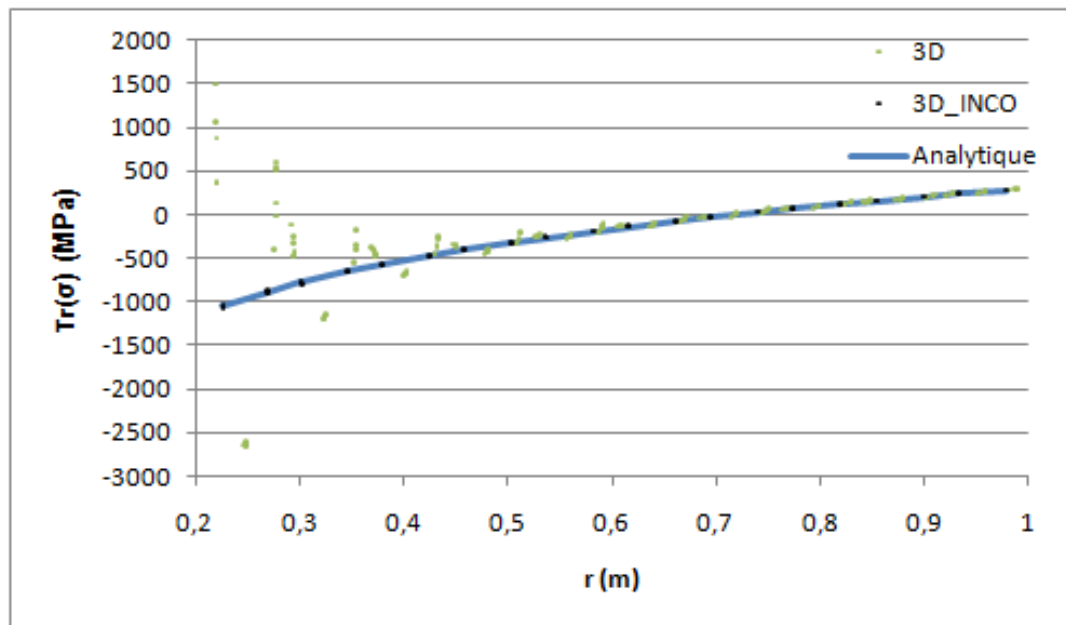
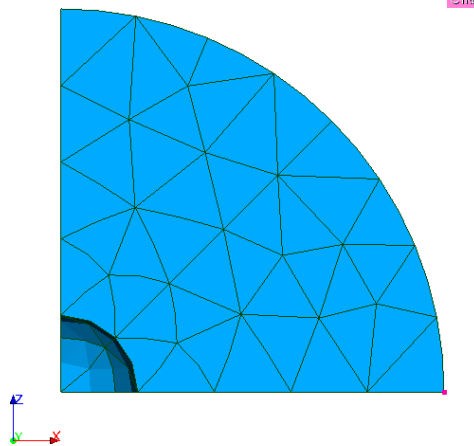


Figure 3.4-a : trace of the constraints in *Mpa* for the formulations 3D, 3D_INCO and the analytical solution

4 Modeling B

4.1 Characteristics of modeling

One takes advantage of symmetries of the problem to model only one eighth of the sphere.



Three modelings are tested: 3D_INCO_UPG (SIMO_MIEHE and GDEF_LOG) and 3D_INCO_UP

4.2 Characteristics of the grid

The grid of 958 nodes contains 535 elements of the type TETRA10.

4.3 Sizes tested and results

One tests the trace of the constraints and the plastic deformation cumulated for the points of the excentré Gauss and excentré.

MODELISATION=' 3D_INCO_UPG ' and DEFORMATION=' SIMO_MIEHE '

Identification	Type of reference	Value of reference	Tolerance
Not the excentré Gauss - $tr \sigma$ - Pa	'ANALYTICAL'	-1054911623.9	0.9%
Not the excentré Gauss - $tr \sigma$ - Pa	'ANALYTICAL'	282824382.06	0.4%
Not the excentré Gauss - p	'ANALYTICAL'	0.10271480980	23%
Not the excentré Gauss - p	'ANALYTICAL'	6.3610302176e ⁻⁵	7.5%

MODELISATION=' 3D_INCO_UPG ' and DEFORMATION=' GDEF_LOG '

Identification	Type of reference	Value of reference	Tolerance
Not the excentré Gauss - $tr \sigma$ - Pa	'ANALYTICAL'	-1055244775.5	0.9%
Not the excentré Gauss - $tr \sigma$ - Pa	'ANALYTICAL'	282824564.66	0.4%
Not the excentré Gauss - p	'ANALYTICAL'	0.10283960537	23%
Not the excentré Gauss	'ANALYTICAL'	6.3609549443e ⁻⁵	7.5%

- p			
-----	--	--	--

MODELISATION=' 3D_INCO_UP' and DEFORMATION=' GDEF_LOG'

Identification	Type of reference	Value of reference	Tolerance
Not the excentré Gauss - $tr\sigma$ - Pa	'ANALYTICAL'	-1055244775.5	0.9%
Not the excentré Gauss - $tr\sigma$ - Pa	'ANALYTICAL'	282824564.66	0.4%
Not the excentré Gauss - p	'ANALYTICAL'	0.10283960537	23%
Not the excentré Gauss - p	'ANALYTICAL'	6.3609549443e ⁻⁵	7.5%

4.4 Remarks

All the incompressible formulations give good performances. One can see on Figure a that one does not have any more oscillations on the value of the trace of the constraints with the incompressible formulations contrary to the standard elements 3D.

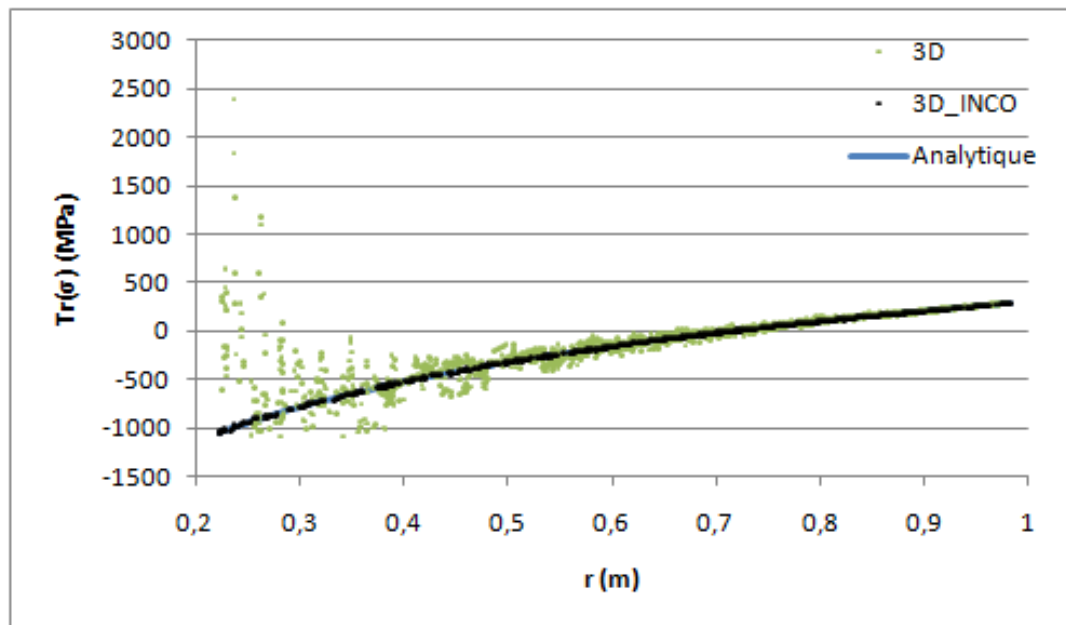
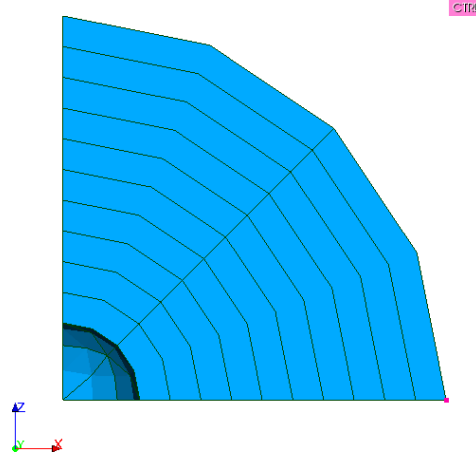


Figure a : Trace of the constraints in *Mpa* for the formulations 3D, 3D_INCO and the analytical solution

5 Modeling C

5.1 Characteristics of modeling

One takes advantage of symmetries of the problem to model only one eighth of the sphere.



Three modelings are tested: 3D_INCO_UPG (SIMO_MIEHE and GDEF_LOG) and 3D_INCO_UP

5.2 Characteristics of the grid

The grid of 279 nodes contains 60 elements of the type PENTA15.

5.3 Sizes tested and results

One tests the trace of the constraints and the plastic deformation cumulated for the points of the excentré Gauss and excentré.

MODELISATION=' 3D_INCO_UPG ' and DEFORMATION=' SIMO_MIEHE '

Identification	Type of reference	Value of reference	Tolerance
Not the excentré Gauss - $tr \sigma$ - Pa	'ANALYTICAL'	-1069165300.4	1%
Not the excentré Gauss - $tr \sigma$ - Pa	'ANALYTICAL'	293654077.71	1%
Not the excentré Gauss - p	'ANALYTICAL'	0.1205244945	17%
Not the excentré Gauss - p	'ANALYTICAL'	2.1945807187e ⁻⁵	1E-5%

MODELISATION=' 3D_INCO_UPG ' and DEFORMATION=' GDEF_LOG '

Identification	Type of reference	Value of reference	Tolerance
Not the excentré Gauss - $tr \sigma$ - Pa	'ANALYTICAL'	-1069097464.2	1%
Not the excentré Gauss - $tr \sigma$ - Pa	'ANALYTICAL'	293654247.5	1%
Not the excentré Gauss - p	'ANALYTICAL'	0.12049702407	17%
Not the excentré Gauss - p	'ANALYTICAL'	2.1945190693e ⁻⁵	1E-5%

MODELISATION=' 3D_INCO_UP' and DEFORMATION=' GDEF_LOG'

Identification	Type of reference	Value of reference	Tolerance
Not the excentré Gauss - $tr\sigma$ - Pa	'ANALYTICAL'	-1069097462.2	1%
Not the excentré Gauss - $tr\sigma$ - Pa	'ANALYTICAL'	293654247.46	1%
Not the excentré Gauss - p	'ANALYTICAL'	0.12049702379	17%
Not the excentré Gauss - p	'ANALYTICAL'	2.1945190811e ⁻⁵	1E-5%

5.4 Remarks

All the incompressible formulations give good performances. One can see on Figure 5.4-a that one does not have any more oscillations on the value of the trace of the constraints with the incompressible formulations contrary to the standard elements 3D.

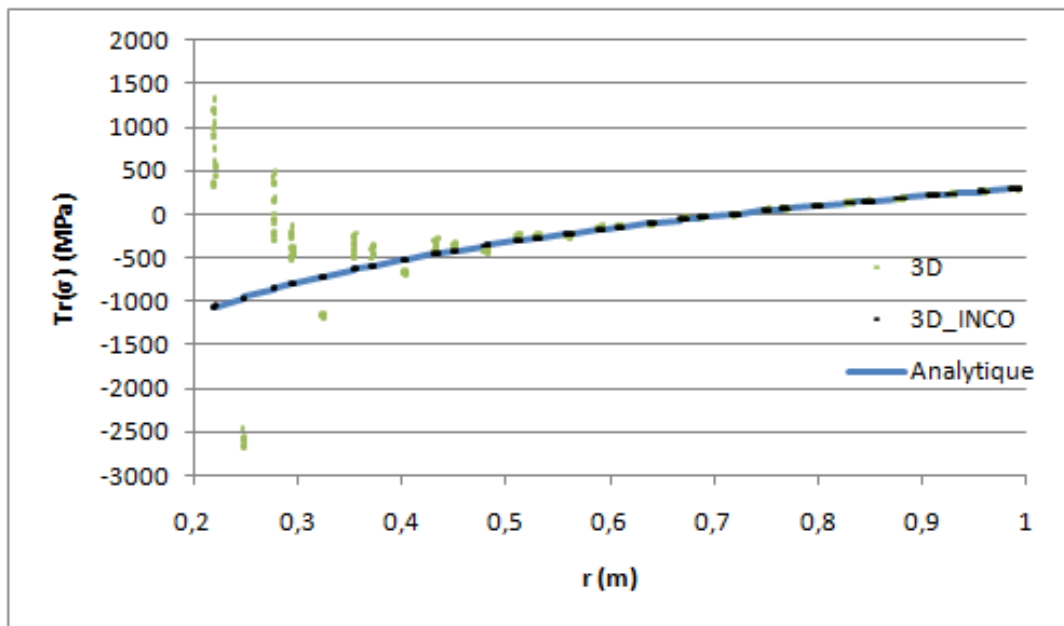
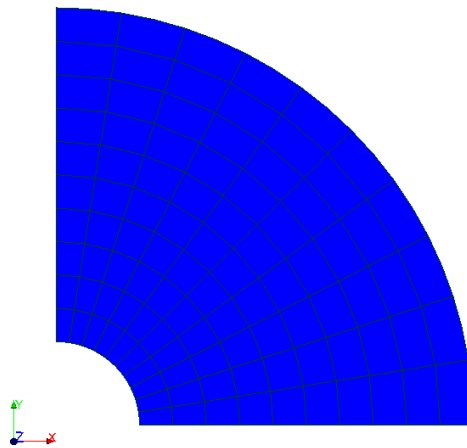


Figure 5.4-a : Trace of the constraints in *Mpa* for the formulations 3D, 3D_INCO and the analytical solution

6 Modeling D

6.1 Characteristics of modeling

One takes advantage of symmetries of the problem to model only one eighth of the sphere.



Three modelings are tested: AXIS_INCO_UPG (SIMO_MIEHE and GDEF_LOG) and AXIS_INCO_UP

6.2 Characteristics of the grid

The grid of 341 nodes contains 100 elements of the type QUAD8.

6.3 Sizes tested and results

One tests the trace of the constraints and the plastic deformation cumulated for the points of the excentré Gauss and excentré.

MODELISATION=' AXIS_INCO_UPG ' and DEFORMATION=' SIMO_MIEHE '

Identification	Type of reference	Value of reference	Tolerance
Not the excentré Gauss - $tr \sigma$ - Pa	'ANALYTICAL'	-1034318375.2	0.2%
Not the excentré Gauss - $tr \sigma$ - Pa	'ANALYTICAL'	284142728.1	0.2%
Not the excentré Gauss - p	'ANALYTICAL'	0.13814566168	32%
Not the excentré Gauss - p	'ANALYTICAL'	5.8228400148e ⁻⁵	46%

MODELISATION=' AXIS_INCO_UPG ' and DEFORMATION=' GDEF_LOG '

Identification	Type of reference	Value of reference	Tolerance
Not the excentré Gauss - $tr \sigma$ - Pa	'ANALYTICAL'	-1034277396.8	0.2%
Not the excentré Gauss - $tr \sigma$ - Pa	'ANALYTICAL'	284142845.29	0.2%
Not the excentré Gauss - p	'ANALYTICAL'	0.13812431142	32%
Not the excentré Gauss - p	'ANALYTICAL'	5.8227926343e ⁻⁵	46%

MODELISATION=' AXIS_INCO_UP' and DEFORMATION=' GDEF_LOG'

Identification	Type of reference	Value of reference	Tolerance
Not the excentré Gauss - $tr\sigma$ - Pa	'ANALYTICAL'	-1034277398.8	0.2%
Not the excentré Gauss - $tr\sigma$ - Pa	'ANALYTICAL'	284142845.27	0.2%
Not the excentré Gauss - p	'ANALYTICAL'	0.13812431254	32%
Not the excentré Gauss - p	'ANALYTICAL'	5.8227926392e ⁻⁵	46%

6.4 Remarks

All the incompressible formulations give good performances. One can see on Figure 6.4-a that one does not have any more oscillations on the value of the trace of the constraints with the incompressible formulations contrary to the standard elements `AXIS`.

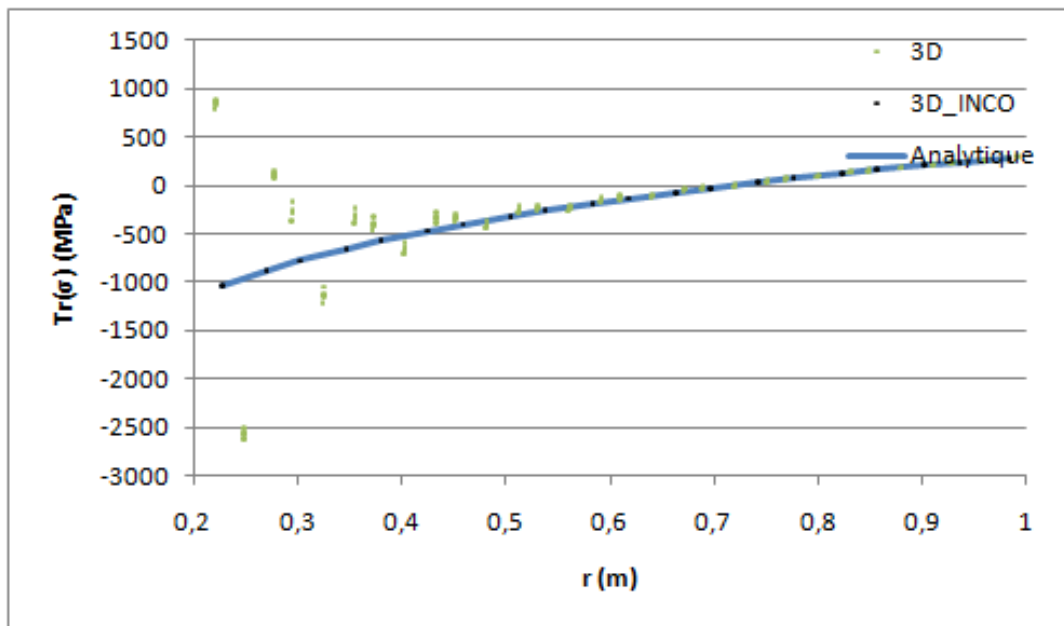
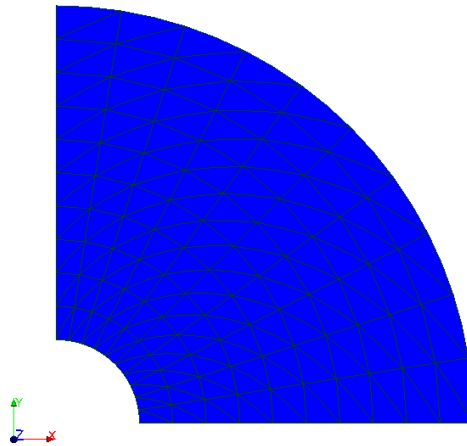


Figure 6.4-a : Trace of the constraints in *Mpa* for the formulations `AXIS`, `AXIS_INCO` and the analytical solution

7 Modeling E

7.1 Characteristics of modeling

One takes advantage of symmetries of the problem to model only one eighth of the sphere.



Three modelings are tested: AXIS_INCO_UPG (SIMO_MIEHE and GDEF_LOG) and AXIS_INCO_UP

7.2 Characteristics of the grid

The grid of 441 nodes contains 200 elements of the type TRIA6.

7.3 Sizes tested and results

One tests the trace of the constraints and the plastic deformation cumulated for the points of the excentré Gauss and excentré.

MODELISATION=' AXIS_INCO_UPG ' and DEFORMATION=' SIMO_MIEHE '

Identification	Type of reference	Value of reference	Tolerance
Not the excentré Gauss - $tr \sigma$ - Pa	'ANALYTICAL'	-1038055558.5	1.5%
Not the excentré Gauss - $tr \sigma$ - Pa	'ANALYTICAL'	287474941.41	0.1%
Not the excentré Gauss - p	'ANALYTICAL'	0.095807224561	16%
Not the excentré Gauss - p	'ANALYTICAL'	4.5056636601e ⁻⁵	10%

MODELISATION=' AXIS_INCO_UPG ' and DEFORMATION=' GDEF_LOG '

Identification	Type of reference	Value of reference	Tolerance
Not the excentré Gauss - $tr \sigma$ - Pa	'ANALYTICAL'	-1036113143.5	1.5%
Not the excentré Gauss - $tr \sigma$ - Pa	'ANALYTICAL'	287474939.50	0.1%
Not the excentré Gauss - p	'ANALYTICAL'	0.096499343842	16%
Not the excentré Gauss - p	'ANALYTICAL'	4.5056643994e ⁻⁵	10%

MODELISATION=' AXIS_INCO_UP' and DEFORMATION=' GDEF_LOG'

Identification	Type of reference	Value of reference	Tolerance
Not the excentré Gauss - $tr\sigma$ - Pa	'ANALYTICAL'	-1036113143.5	1.5%
Not the excentré Gauss - $tr\sigma$ - Pa	'ANALYTICAL'	287474939.50	0.1%
Not the excentré Gauss - p	'ANALYTICAL'	0.096499343739	16%
Not the excentré Gauss - p	'ANALYTICAL'	4.5056643999e ⁻⁵	10%

7.4 Remarks

All the incompressible formulations give good performances. One can see on Figure 7.4-a that one does not have any more oscillations on the value of the trace of the constraints with the incompressible formulations contrary to the standard elements `AXIS`.

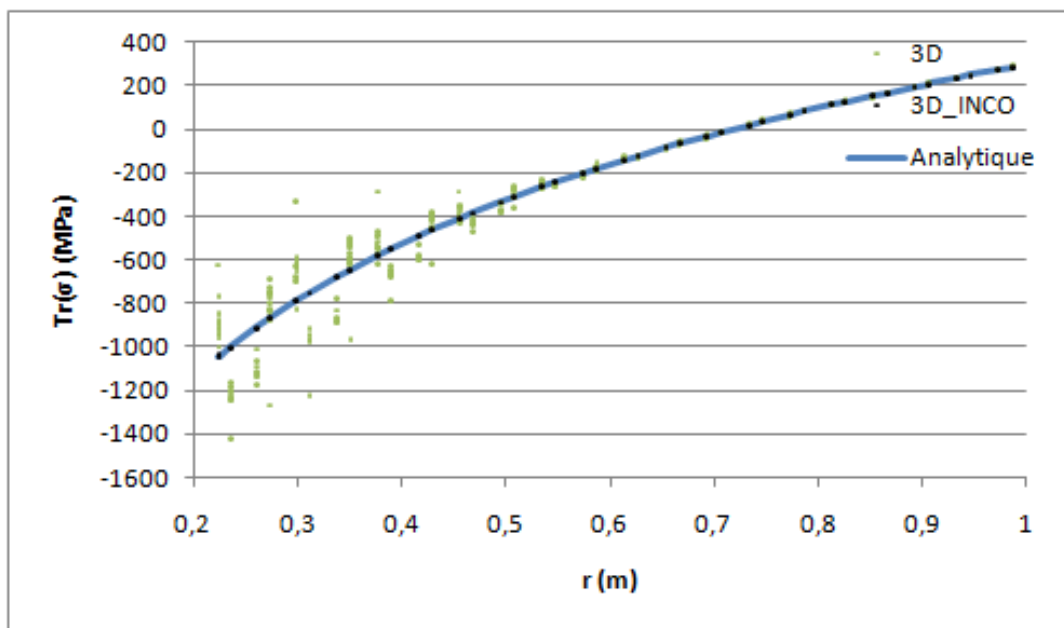


Figure 7.4-a : Trace of the constraints in *Mpa* for the formulations `AXIS`, `AXIS_INCO` and the analytical solution

8 Summary of the results

The got results show that the incompressible formulations make it possible to control well the phenomena of oscillations of the trace of the constraints in great deformations.